Nanoscale

Volume 1 | Number 1 | Jan 2013 | Pages 1–100

Nanoscale

www.rsc.org/nanoscale

ROYAL SOCIETY OF CHEMISTRY

ROYAL SOCIETY OF CHEMISTRY

www.rsc.org/nanoscale

1   Titanium dioxide nanoparticles alter the cellular morphology via

2   disturbing their microtubule dynamics

3   Zhilei Mao [a, b,1], Bo Xu [a, b, 1], Xiaoli Ji [a, b,1], Kun Zhou [a, b], Xuemei Zhang [a, b] Minjian

4   Chen [a, b], Xiumei Han [a, b], Qiusha Tang [c], , Xinru Wang [a, b], Yankai Xia [a, b, *]

5   [a] State Key Laboratory of Reproductive Medicine, Institute of Toxicology, Nanjing

6   Medical University, Nanjing 211100, China

7   [b] Key Laboratory of Modern Toxicology of Ministry of Education, School of Public

8   Health, Nanjing Medical University, Nanjing 211100, China

9   [c] Medical School, Southeast University, Nanjing, Jiangsu 210009, China;

10   [1] The authors contributed equally.

11   [*] **To whom correspondence should be addressed:**

12   Yankai Xia, Ph.D.

13   State Key Laboratory of Reproductive Medicine, Institute of Toxicology,

14   Nanjing Medical University, 101 Longmian Road, Nanjing 211100, China.

15   Tel: +86-25-86868425   Fax: +86-25-86868427

16

17

18 **Abstract**

19 Titanium dioxide (TiO_2) nanoparticles (NPs) have been widely used in our daily lives

20 such as in the areas of sunscreens, cosmetics, toothpastes, food products, and

21 nanomedical reagents. Recently increasing concerns have been raised about their

22 neurotoxicity, but the mechanisms underlying such toxic effects are still unknown. In

23 this work, we employed a human neuroblastoma cell line (SH-SY5Y) to study the

24 effects of TiO_2 NPs on neurological system. Our results showed that TiO_2 NPs did not

25 affect cell viability but induced noticeable morphological changes until 100μg/ml.

26 Immunofluorescence detection showed disorder, disruption, retraction, and decreased

27 intensity of the microtubules after TiO_2 NPs treatment. Both α and β tubule

28 expression did not change in the TiO_2 NPs-treated group, but the percentage of

29 soluble tubule was increased. Microtubule dynamic study in living cells indicated that

30 TiO_2 NPs caused a lower growth rate and a higher shortening rate of microtubule as

31 well as shortened life time of *de novo* microtubules. TiO_2 NPs did not cause changes

32 in the expression and phosphorylation state of tau proteins, but tau-TiO_2 NPs

33 interaction was observed. TiO_2 NPs could interact with tubule heterodimers,

34 microtubules and tau proteins, which lead to the instability of microtubules, thus

35 contributing to the neurotoxicity of TiO_2 NPs.

36 **Introduction**

37 Owing to the excellent physicochemical properties, TiO_2 NPs were widely used in

38 aeronautical materials, implanted biomaterials, paints, paper, sunscreens, and food

39   products. Current studies mainly focus on its new applications in biochemistry as well

40   as in other industry fields[1-3]. Increasing concerns have been raised recently about the

41   safety of such NPs[4, 5]. It is urgent to gain more information about this material in this

42   regard, given that little mechanistic or theoretic studies were put forward in this field.

43   TiO_2 NPs enters human body via occupational inhalation, bio-medical ceramic

44   injection, biomaterials implantation and food exposure[5]. They could pass through

45   blood-brain barrier (BBB)[6, 7] and induce oxidative damage, inflammatory responses

46   and impair spatial recognition memory in adult mice[8, 9]. Furthermore, they could

47   penetrate placental barrier to the fetal mice and affect their cranial nerve system[10, 11].

48   A range of studies also showed their affects on neurons and glial cells[12-14], but no

49   mechanistic work was described in the literature. So our work carried out around TiO_2

50   NPs' bio-effects on nervous system.

51   Microtubule plays an important role in neuronal cells, including information

52   carrying[15], neurodevelopment[16], migration[17] and so on. The GTP-tubule added to the

53   plus end of microtubule and GDP-tubule depolymerized from the minus end which is

54   called "dynamic instability"[18]. This progress was affected by tubule concentration,

55   GTP, microtubule-associated proteins (MAPs) and so on[19], and it plays a crucial role

56   in neuronal morphogenesis[20]. TiO_2 NPs-microtubule interaction has been studied *in*

57   *vitro* previously[21], but whether TiO_2 NPs could interact with microtubules in living

58   cells is still unknown.

59 NPs-protein interactions were mostly studied *in vitro* or by computational simulation

60 study[22]. *In vivo* studies are hard to be carried out due to the limitation of current

61 technologies and methods, so the safety evaluation of thousands of nanoparticles in

62 living things is a big problem. Though we usually analyze the interactions based on

63 co-localization, Xia et al[23] showed that fluorescence-labelled TiO_2 NPs localized in

64 late endosomal without eliciting any noticeable effects, which meant that

65 co-localization was not in agreement with interaction. Here we utilize human

66 neuroblastoma cell line (SH-SY5Y) as a proper model to study the behaviors of TiO_2

67 NPs in living cells via the functional alteration of some proteins.

68 **Results and Discussion**

69 **Characterization of TiO_2 NPs**

70 The characteristics of TiO_2 NPs in cell culture medium were presented in Figure 1A.

71 Transmission electron microscope (TEM) demonstrated that TiO_2 NPs were nearly

72 spherical (Figure 1B), with a particle size of 20.90±3.57 nm, which was similar to the

73 manufacturer reported size (~21nm). The particle size distribution (Figure 1C)

74 showed that TiO_2 NPs had a narrow particle-size distribution from 100-150 nm in

75 culture medium. And the dynamic light scattering (DLS) results exhibited that TiO_2

76 NPs aggregated in the culture medium with a larger hydrodynamic diameter of

77 110.0±72.9 nm, but had a better dispersion in medium than in water (Figure S1),

78 which might attribute to serum proteins for the better dispersion[24]. The zeta potential

79   of the TiO$_2$ NPs was -0.73±1.27 mV in cell culture medium, whereas it was lower in

80   water (-142.56±19.80 mV), which might also be the result of protein absorption[25].

81   **TiO$_2$ NPs enter SH-SY5Y cells and change their morphology**

82   SH-SY5Y cells were treated with various concentrations of TiO$_2$ NPs (0.1, 1, 10, 100

83   μg/ml) for 24h, and cell viability was determined by MTT (Figure 2A). Cell viability

84   was not affected under the concentrations of TiO$_2$ NPs administered. As shown in

85   Figure 2B, at the highest concentration, the morphology of nearly 50% cells changed

86   from a flat polygon with synapses to a cobble stone-like morphology, and their axons

87   dispersed or drew back. Therefore, we used and focused on the highest dose group to

88   explore the mechanisms underlying the morphological changes.

89   To confirm the morphological changes were caused by TiO$_2$ NPs, the uptake of NPs

90   were assessed by Flow cytometry (FCM) and TEM. Figure 2C showed that the uptake

91   of TiO$_2$ was in a dose-dependent manner. With the increasing of TiO$_2$ NPs

92   concentrations, cell size and intracellular density increased accordingly. TEM

93   imaging of a SH-SY5Y cell treated with TiO$_2$ NPs (Figure 2D) showed that most of

94   the TiO$_2$ NPs accumulated in the cytoplasm and lysosomes, not in the nucleus, which

95   was consistent with previous studies[26].

96   **ROS doesn't play a key role in the morphology change caused by TiO$_2$ NPs**

97   Many NPs exert their effects by producing reactive oxygen species(ROS)[27], which

98   could affect microtubules dynamics[28], and finally change cell morphology or remodel

99   microtubule network[29, 30]. This raised our interest whether ROS plays a key role in the

100   morphological changes. Our results showed that TiO_2 NPs could increase ROS

101   generation significantly in SH-SY5Y cells at the highest concentration (Figure 2E).

102   Incubate with 20 μM ROS scavengers N-acetyl cysteine (NAC) for 24 h could abolish

103   the TiO_2 NPs induced elevation of ROS (Figure 2F). However, the morphological

104   changes were not reversed (Figure 2G), indicating that ROS was not a key factor here.

105   **TiO_2 NPs change the microtubule network of SH-SY5Y cells**

106   Microtubule plays an important role in the shape maintenance of cells, so we wonder

107   whether TiO_2 NPs acted on microtubule network. Microtubules were examined by

108   immunofluorescence with α-tubule antibody and confocal microscope. Figure 3A

109   showed that, compared with the control group, microtubules of the treated cells were

110   noticeably drew back and winding, and their density decreased apparently. In addition,

111   the arrangement of microtubules was in disorder. They abrogated the formation of

112   long and extended microtubules, and microtubule network was significantly

113   remodeled

114   **TiO_2 NPs do not affect the expression of α and β tubules**.

115   The concentrations of available tubule heterodimers have an impact on growth speed

116   and persistence of microtubules, and eventually affect microtubule network[31].

117   Previous studies have reported that TiO_2 NPs reduced α-tubule and β-tubule levels in

118   Arabidopsis thaliana and disrupted microtubule[32]. And an *in vitro* model also showed

119   that TiO_2 NPs could interact with DNA[33]. To examine whether the changes of cell

120   morphology and cytoskeleton were caused by the TiO_2 NPs-DNA interaction and

121   decreased levels of tubule heterodimers, we investigated the expression level of two

122   main microtubule proteins, α-tubule and β-tubule by Western blotting. We found that

123   neither α-tubule nor β-tubule expression level was changed (Figure 3B), indicating

124   that α-tubule and β-tubule expression was not related to the disrupted microtubule

125   networks. This result was consistent with the distribution of TiO_2 NPs, as TiO_2 NPs

126   were not identified in cell nucleus of SH-SY5Y. Therefore, it is warranted to study the

127   microtubule dynamics.

128   **TiO_2 NPs change the ratio of polymerized to soluble tubule**

129   The ratio of polymerized and depolymerized tubule changes when the microtubule

130   dynamics lose balance. So we studied the polymerized and depolymerized tubules

131   ratios in both control cells and TiO_2 NPs-treated cells. Figure 3C and 3D showed that,

132   the majority of tubules were found in the soluble form, and the ratio of polymerized

133   (P) to soluble (S) tubule was nearly 2:3 in control cells. In contrast, in TiO_2

134   NPs-treated cells, although the majority of tubule was still in soluble form, the ratio of

135   polymerized to soluble tubule was decreased dramatically (1:5), indicating that TiO_2

136   NPs changed the microtubule dynamics. But how does this change happen and which

137   procedure(s) of microtubule dynamics was(were) affected are still unknown.

138   **TiO_2 NPs disturb microtubule dynamic *in vivo***

139   To further investigate the effects of TiO_2 NPs on microtubule dynamics, we

140   transfected cells with virus carrying end-binding-protein 3 fused with green

141   fluorescent protein (EB_3-GFP), which facilitated the study of microtubule dynamics

142   with confocal microscope in living cells. We evaluated several indexes of microtubule

143   dynamics including microtubule growth speed, shortening speed, trajectory of

144   newborn microtubules, life time and length distribution of unbroken microtubules.

145   TiO_2 NPs decreased microtubules growth speed significantly, 343.6±82.8 nm/s in

146   control cells vs 223.2±69.5 nm/s in treated cells ($P<0.01$). *In vitro* studies have

147   reported that TiO_2 NPs could bind to the tubule surface via forming hydrogen bond or

148   electrostatic interaction, which changes their 3D structures and finally affects

149   microtubule dynamics[21, 34]. Also in the perspective of quantum biology, molecules

150   interact with each other via their surface electrons, this interaction finally change the

151   structures of both, such as the enzyme and substrate interaction. TiO_2 NPs possess

152   surface charge as measured with zeta potential, which gives them the ability to

153   interact with proteins. Previous study showed that the same nanoparticle cores with

154   the same hydrodynamic size led to big differences in protein absorption and cell

155   uptake[35] by functionalization with opposite surface charge. This emphasizes the

156   importance of surface charge on the bio-effects of NPs, different charges gave them

157   different characteristics. Our results together with previous studies indicated that TiO_2

158   NPs could and may absorb to tubule heterodimers in living cells, interact with their

159   protein corona, change their spatial structures and decrease the effective concentration

160   of tubule heterodimers, and contributed a lower growth speed.

161   We next measured the shortening rate, the result showed that shortening rate also

162   changed significantly (81.9±30.2 nm/s in control cells, and 332.4±117.1 nm/s in

163   treated cells ($P < 0.01$)). This alteration meant that microtubules were under instability

164   conditions, indicating that TiO_2 NPs could also interact with assembled microtubules.

165   When TiO_2 NPs get close to assembled microtubules, their surface charge disturbed

166   the normal electronic environment needed to sustain microtubule structures, in turn,

167   microtubules were easy for degeneration. The normal electronic environment includes

168   hydrogen bonding, Van der Waals' force and so on. Our results are in agreement with

169   those by Ojeda-Lopez and his colleges[36], who discovered that a highly charged small

170   molecule could cause shape transformation of taxinol stabilized microtubules over the

171   surface charge interaction. And a recent work in Science also announced the effect of

172   GTP-GDP transformation on microtubule depolymerization in quantum biology[37],

173   which emphasised the effects of normal electronic environment changing on

174   maintaining the microtubules. According to these theories, microtubules are expected

175   to be hard for persistent growth and tend to be shorter in length in the presence of NPs.

176   We then recorded the trajectory of *de novo* microtubules in living cells by confocal

177   microscope during about 2 min. As presented in Figure 4A, most of the *de novo*

178   microtubules in control cells are found to be longer, successive and irradiate from

179   centrosome to cell margin. In contrast, nascent microtubules in TiO_2 NPs-treated cells

180   were obviously short and in disorder (supplementary Movies S1 and S2; S1: Control,

181   S2: TiO_2 treated). Figure 4B showed the histogram of the length distribution of

182   unbroken microtubules in two groups. Microtubules in control group with a length

183   (3110.0±1586.5 nm) are significantly longer than that those in treated group

184   (1627.8±820.1 nm) ($P < 0.01$), and their life times (duration from merging to

185   dismissing) were further calculated (Figure 4C). Life time decreased from 44.9±12.5 s

186   in control cells to 17.47±6.5 s in treated cells significantly ($P < 0.01$). All these results

187   showed that TiO$_2$ NPs affected not only existed microtubules, but also *de novo*

188   microtubules, and supported our hypothesis.

189   We also monitored the average fluorescence intensity of both TiO$_2$ NPs-treated and

190   untreated cells for 24 h to evaluate microtubule steady state. With time, average

191   fluorescence intensity decreased in both groups, but the alternation of fluorescence

192   intensity in the two groups was different ($P < 0.05$). Average fluorescence intensity of

193   NPs-treated cells began to decrease from the 5th h, and kept decreasing until 12th h,

194   and then reached and maintained at a new stage (Figure 4D). Such results suggest that

195   TiO$_2$ NPs brought the microtubule dynamics to a new equilibrium, which may result

196   from decreased growth rate and increased shortening rate.

197   Now more researches indicated that nanoparticle could interact with microtubules,

198   and affected microtubule dynamics[38], even inorganic nanoparticle could bind to

199   microtubules for cancer therapy[39]. Further study of TiO$_2$ NPs in the perspective of

200   quantum biology might help us to find the binding sites of on microtubules according

201   to their surface charges or modified surface someday, or predict the potential NPs

202   may target on microtubules.

203   **Tau proteins are responsible for TiO$_2$ NPs-induced neurotoxicity**

204   Tau proteins are microtubule-associated proteins (MAPs) that are highly expressed in

205   neurons where they play an important role in microtubule polymerization, stable

206   maintenance, axon growth and function maintenance[40]. We tested whether tau plays a

207   role in the microtubule dynamic disruption caused by TiO_2 NPs. In our study, neither

208   the mRNA or protein expression of tau changed after TiO_2 NPs exposure (Figure 5A).

209   The phosphorylation of tau at two sites, Ser202 and Ser396, which is considered to

210   modulate the ability of tau of binding and stabilizing microtubules[41, 42] didn't show

211   any difference(Figure 5B) between control and treated cells. TiO_2 NPs showed strong

212   ability of protein adsorption in a range of NPs[43]. We wonder whether TiO_2 NPs

213   absorb tau proteins and prevent them from binding to the proper position of

214   microtubule to exert their functions. Examined by Western blotting, the result showed

215   that the level of total tau was significantly lower in TiO_2 NPs-treated group (Figure

216   5C), indicating the existence of tau-NPs interaction in living cells, which could

217   partially explain the specific neurotoxicity of TiO_2 NPs. Compared with GAPDH we

218   knew not every protein could interact with TiO_2 NPs. The interaction between NPs

219   and protein might be related to their surface charge or protein structures.

220   **Conclusion**

221   In this work, we explored the mechanisms of TiO_2 NPs induced morphological

222   changes in living cells, and for the first time tried to explain the bio-effects of TiO_2

223   NPs from the point view of quantum biology. A brief summary of our research was

224   outlined in Figure 6A. TiO_2 NPs entered cells, interacted with tubule heterodimers,

225 assembled microtubules and tau proteins, which led to the dysfunction of microtubule

226 dynamics. Above all, we proposed the TiO_2 NPs-microtubule-tau interaction model in

227 Figure 6B. In the normal condition, tubule heterodimers add to the plus end of

228 microtubule and depolymerize from the minus end. Tau proteins bind to the proper

229 sites of microtubules, promoting assemble and stabilizing nascent microtubules.

230 While in the presence of TiO_2 NPs, NPs interact with tubule heterodimers, change

231 their normal structure and prevent them from polymerization. Alternatively, they

232 could interact with assembled microtubules, change the normal electronic

233 environment via their surface charging, thus leading to instable microtubules and

234 shorten their life time. Moreover, tau proteins are absorbed by TiO_2 NPs, which might

235 prevent them from performing their functions and facilitate the aggravation of those

236 instable microtubules. TiO_2 NPs might be a contributing factor of tau or microtubule

237 disability disease. It is also possible that TiO_2 NPs may have potential therapeutic

238 value in curing neurologic tumors.

239 **Experimental**

240 **The characteristics and dispersion of TiO_2 NPs**

241 TiO_2 NPs (Sigma-Aldrich, 13463-67-7, 21nm) were characterized in distilled and

242 deionized water and in complete cell culture medium supplemented with 10% fetal

243 bovine serum (FBS). For better dispersion, suspensions were vortex mixed at high

244 speed for 1 min, sonicated in ice water bath (100 W, 30 min) for two cycles. TEM

245 images of NPs were obtained by a JEOL JEM 2100 transmission electron microscope

246   operating at 120 kV. Dynamic light scattering (DLS) analysis was performed to

247   determine size distributions and hydrodynamic diameters of NPs in water and cell

248   culture medium, respectively, and zeta potential was analyzed in a Zetasizer Nano

249   series model ZS (Brookhaven Instrument Corp).

250   For cell treatment, TiO_2 NPs were sterilized by ultraviolet and suspended in cell

251   culture medium at a concentration of 1 mg/ml, mixed and sonicated as described

252   above. A range of concentrations of TiO_2 NPs were diluted and sonicated for another

253   30 min before use.

254   **Cell culture**

255   SH-SY5Y cells (CRL-2266[TM]) were purchased from American Type Culture

256   Collection (ATCC, Manassas VA, USA) and cultured in Dulbecco's Modified Eagle's

257   Medium (Hyclone, UT, USA) supplemented with 10% FBS, 100 U/ml penicillin, and

258   100 μg/ml streptomycin at 37°C, 5% CO_2. Medium was replaced every day. Nikon

259   light microscope (ECLIPSE, TS100, Japan) was used to observe cell morphology.

260   Images were obtained using a Leica DFC290 HD camera.

261   **Cell viability**

262   Cells were seeded on 96-multiwell plates and cultured with different concentrations

263   (0.1, 1, 10, 100 μg/ml) of TiO_2 NPs for 24h. After incubation, 20 μl of 5mg/ml

264   3-(4,5-Dimethylthiazol-2-yl)-2,5-diphenyltetrazolium bromide (MTT) stock solution

265   was added per well and incubated for another 3 h. 200 μl of DMSO was added after

266 the medium was removed, and incubated for another 10 min at 37°C. The supernatant

267 absorbance was measured at 490 nm on a UV/vis spectrometer (Ocean Optics,

268 HR4000). Each assay was repeated three times independently.

269 **The uptake of TiO2 NPs**

270 Cells were seeded in 10-cm dishes, treated with a range of concentrations of TiO$_2$ NPs.

271 After 24 h incubation, TiO$_2$ NPs uptake was evaluated by FCM (BD FACSCalibur,

272 USA) as previously reported[44] and by TEM. For FCM analysis, cells were washed

273 twice mildly with PBS and resuspended with 1 ml PBS after trypsin digestion.

274 Forward-scatter(ed) (FS) light and side scatter(ed) (SS) light were analyzed using

275 FCM. For TEM analysis, cells were collected and fixed with 1% glutaraldehyde in

276 0.12M phosphate buffer, washed with phosphate buffer. 1% buffered osmium

277 tetroxide was used for post-fixation, and dehydrated in a graded acetone series. After

278 embedded in Araldite, samples were stained with lead citrate and uranyl acetate.

279 **Analysis of reactive oxygen species (ROS)**

280 ROS was detected by Reactive Oxygen Species Assay Kit (Beyotime, China). The

281 cells were seeded in 10-cm dishes and treated with a range of concentrations of TiO$_2$

282 NPs. After 24 h treatment, cells were collected and incubated with DCFH-DA for

283 another 20 min, then washed three times with PBS and measured with FCM at 488

284 nm excitation.

285 **Confocal microscope examination**

286   Cells were seeded in glass bottom dishes (In vitro scientific), treated with 100μg/ml

287   TiO$_2$ NPs for 24 h, and fixed with 4% paraformaldehyde for 30 min. Cytoskeleton

288   was revealed by anti-α-tubule antibody (1:200, Beyotime), combined with a

289   secondary goat anti-mouse IgG antibody conjugated with FITC (1:200, Beyotime).

290   Nucleus was stained with DAPI (1:1000, Beyotime). Images were obtained by Nikon

291   E800 confocal microscope (Nikon, Japan).

292   **Protein preparation and western blotting assay**

293   Cells were resuspended in ice-cold RIPA buffer (Beyotime, China) containing 1%

294   PMSF (Beyotime, China) after 24 h incubation with TiO$_2$ NPs, and lysed on ice for 30

295   min. After centrifugation at 1000 rpm for 10 min, supernatant was collected as the

296   total proteins and the concentrations were determined using BCA Protein Assay Kit

297   (Beyotime, China).

298   For western blotting assay, 80μg of total proteins were loaded to 10% SDS

299   polyacrylamide gel electrophoresis (SDS-PAGE). Antibodies used were anti α-tubule

300   (Beyotime, 1:1000), anti β-tubule (Beyotime,1:1000), total tau (Epitomics, 1:1000),

301   anti GAPDH (Beyotime, 1:1000), anti-Tau (phospho S$_{202}$) antibody (Epitomics,

302   1:1000), anti-Tau (phospho S$_{396}$) antibody (Epitomics, 1:1000), with the secondary

303   goat anti-mouse IgG conjugated with HRP and goat anti-rabbit IgG conjugated with

304   HRP. Each blot was repeated three times.

305   **Isolation of polymerized and depolymerized microtubules**

306 Proteins were exacted as previously described[45]. Briefly, after treated with TiO_2 NPs,

307 cells were washed three times with PBS. 100 μl of hypotonic buffer (1mM $MgCl_2$,

308 2mM EGTA, 0.5% NP-40, 1.3% cocktail, 1mM orthovanadate and 20mM Tris–HCl,

309 pH6.8) was added, and cells were scraped and collected into a 1.5ml tube, and lysed

310 at $37^{\circ}C$ for 5 min protected from light. After vortex, samples were centrifuged at

311 14000g for 10 min. The supernatants containing depolymerized tubule were

312 transferred to another tube and equivalent amount of buffer was added to resuspend

313 the pellets. Equal volumes of the lysates in each group were used for Western analysis

314 with anti α-tubule antibody. Densitometry was performed using image-J software.

315 *In vivo* **microtubule dynamics study**

316 Microtubule dynamics are visualized in living cells via a series of proteins[46-48]. In this

317 work, we used end-binding-protein 3 fused with GFP (EB_3-GFP) to study the

318 microtubule dynamics as previous described[49]. Lentiviral vectors express EB3-GFP

319 proteins were purchased from GENECHEM (shanghai, China) and operated following

320 the protocol. Briefly, cells were seeded in a proper density; virus and enhanced

321 infection solution were added. Medium was refreshed after 12 h infection, and cells

322 were continuously cultured until the third day. The transfected cells can highly

323 express EB_3-GFP proteins at least two weeks. The microtubule dynamics were

324 analyzed in control cells (20 cells) and NPs-treated cells (20 cells) as previously

325 reported[50]. Images (512×512) were collected every 1.96 sec without interval and

326 totally 100 pictures were collected. Growth speed and shortening speed were

327 measured as displacement of the microtubule end divided by the time between

328 successive images (3-5 sec) in a time-lapse series. Trajectory, life time and length

329 distribution were performed on the projection images.

330 **24 h dynamic monitoring**

331 After transfected with EB_3-GFP vectors, cells were seeded in 96 multi-well plates,

332 administrated with TiO_2 NPs and the average fluorescence intensity was monitored

333 successively for 24 h with high content screening assay[51]. Simply, 36 random insights

334 were chosen, signals and images were collected per hour for 24 h using a ×20

335 microscope objective. Cells were located by nuclei stained with Hoechst 33342

336 (Beyotime, China). Images and data were automatically obtained from KineticScan[TM]

337 Reader (KSR; Cellomics, Pittsburgh, USA). Cell counts were utilized to control the

338 effect of cell proliferation. The Cell Health Profiling BioApplication (Cellomics,

339 Pittsburgh, USA) was used to acquire and analyze the images. These experiments

340 were carried out three times independently.

341 **RNA isolation and quantitative real-time PCR assay**

342 Cells were treated and collected, total RNA was extracted using TRIzol reagent

343 (Invitrogen, Carlsbad, CA) according to the instructions. RNA concentration was

344 determined by measuring the absorbency at 260 nm. cDNA was prepared according to

345 the regent kits (Takara, Tokyo, Japan). Real-time PCR reactions were carried out on

346 ABI7900 Fast Real-Time System (Applied Bio systems, Foster city, CA, USA).

347   Primers for tau were synthesized by Invitrogen (Shanghai) as follows, Forward primer:

348   GGAGAAGTGGTCTAGCAAGATCG, Reverse primer:

349   AGAAACGCACCTCCACCATTC.

350   **TiO$_2$ NPs and tau proteins interaction assay**

351   To ensure that TiO$_2$ NPs interact with tau proteins in living cells, cells were seeded in

352   10-cm dishes, and when reached 80% confluences, they were treated with TiO$_2$ NPs

353   for 24 h. Both the treated and control cells were lyzed and centrifugated at 1000g for

354   10 min. The supernatant was analyzed by the BCA Protein Assay Kit as total fraction

355   (Beyotime, China), and adjusted to the same content. Equal volumes of the samples

356   were centrifugated at 16000g for 20 min[43]. Supernatants were collected and loaded for

357   Western assay.

358   **Competing interests**

359   The authors declare no conflict of interest.

References

368   1.   M. N. Hyder, B. M. Gallant, N. J. Shah, Y. Shao-Horn and P. T. Hammond,

369   *Nano letters*, 2013, 13, 4610-4619.

370   2.   V. Singh, I. J. Beltran, J. C. Ribot and P. Nagpal, *Nano letters*, 2014, 14,

371   597-603.

372   3.   S. J. Yuan, J. J. Chen, Z. Q. Lin, W. W. Li, G. P. Sheng and H. Q. Yu, *Nature*

373   *communications*, 2013, 4, 2249.

374   4.   G. J. Nohynek and E. K. Dufour, *Archives of toxicology*, 2012, 86, 1063-1075.

375   5.   M. Skocaj, M. Filipic, J. Petkovic and S. Novak, *Radiology and oncology*,

376   2011, 45, 227-247.

377   6.   P. J. Borm, D. Robbins, S. Haubold, T. Kuhlbusch, H. Fissan, K. Donaldson,

378   R. Schins, V. Stone, W. Kreyling, J. Lademann, J. Krutmann, D. Warheit and

379   E. Oberdorster, *Particle and fibre toxicology*, 2006, 3, 11.

380   7.   A. Peters, B. Veronesi, L. Calderon-Garciduenas, P. Gehr, L. C. Chen, M.

381   Geiser, W. Reed, B. Rothen-Rutishauser, S. Schurch and H. Schulz, *Particle*

382   *and fibre toxicology*, 2006, 3, 13.

383   8.   J. Wang, Y. Liu, F. Jiao, F. Lao, W. Li, Y. Gu, Y. Li, C. Ge, G. Zhou, B. Li, Y.

384   Zhao, Z. Chai and C. Chen, *Toxicology*, 2008, 254, 82-90.

385   9.   R. Hu, X. Gong, Y. Duan, N. Li, Y. Che, Y. Cui, M. Zhou, C. Liu, H. Wang

386   and F. Hong, *Biomaterials*, 2010, 31, 8043-8050.

387   10.   M. Umezawa, H. Tainaka, N. Kawashima, M. Shimizu and K. Takeda, *The*

388   *Journal of toxicological sciences*, 2012, 37, 1247-1252.

389   11.   K.-i. S. Ken Takeda, Aki Ishihara,Miyoko Kubo-Irie,Rie Fujimoto,Masako

390   Tabata, Shigeru Oshio, Yoshimasa Nihei, Tomomi Ihara, Masao Sugamata,

391   *Journal of Health Science*, 2009, 8.

392   12.   T. C. Long, N. Saleh, R. D. Tilton, G. V. Lowry and B. Veronesi,

393   *Environmental science & technology*, 2006, 40, 4346-4352.

394   13.   S. G. Marquez-Ramirez, N. L. Delgado-Buenrostro, Y. I. Chirino, G. G.

395   Iglesias and R. Lopez-Marure, *Toxicology*, 2012, 302, 146-156.

396   14.   V. Valdiglesias, C. Costa, V. Sharma, G. Kilic, E. Pasaro, J. P. Teixeira, A.

397   Dhawan and B. Laffon, *Food and chemical toxicology : an international

398   journal published for the British Industrial Biological Research Association*,

399   2013, 57, 352-361.

400   15.   E. W. Dent and P. W. Baas, *Journal of neurochemistry*, 2014, 129, 235-239.

401   16.   M. Breuss and D. A. Keays, *Advances in experimental medicine and biology*,

402   2014, 800, 75-96.

403   17.   Q. Wu, J. Liu, A. Fang, R. Li, Y. Bai, A. R. Kriegstein and X. Wang,

404   *Advances in experimental medicine and biology*, 2014, 800, 25-36.

405   18.   M. W. Kirschner and T. Mitchison, *Nature*, 1986, 324, 621.

406   19.   B. van der Vaart, A. Akhmanova and A. Straube, *Biochemical Society

407   transactions*, 2009, 37, 1007-1013.

408   20.   A. Sakakibara, R. Ando, T. Sapir and T. Tanaka, *Open biology*, 2013, 3,

409   130061.

410   21.   Z. N. Gheshlaghi, G. H. Riazi, S. Ahmadian, M. Ghafari and R. Mahinpour,

411   *Acta biochimica et biophysica Sinica*, 2008, 40, 777-782.

412   22.   S. R. Saptarshi, A. Duschl and A. L. Lopata, *Journal of nanobiotechnology*,

413   2013, 11, 26.

Nanoscale Accepted Manuscript

414   23.   T. Xia, M. Kovochich, M. Liong, L. Madler, B. Gilbert, H. Shi, J. I. Yeh, J. I.

415   Zink and A. E. Nel, *ACS nano*, 2008, 2, 2121-2134.

416   24.   Z. Ji, X. Jin, S. George, T. Xia, H. Meng, X. Wang, E. Suarez, H. Zhang, E. M.

417   Hoek, H. Godwin, A. E. Nel and J. I. Zink, *Environ Sci Technol*, 2010, 44,

418   7309-7314.

419   25.   Z. E. Allouni, M. R. Cimpan, P. J. Hol, T. Skodvin and N. R. Gjerdet,

420   *Colloids and surfaces. B, Biointerfaces*, 2009, 68, 83-87.

421   26.   Z. E. Allouni, P. J. Hol, M. A. Cauqui, N. R. Gjerdet and M. R. Cimpan,

422   *Toxicology in vitro : an international journal published in association with*

423   *BIBRA*, 2012, 26, 469-479.

424   27.   I. Pujalte, I. Passagne, B. Brouillaud, M. Treguer, E. Durand, C.

425   Ohayon-Courtes and B. L'Azou, *Particle and fibre toxicology*, 2011, 8, 10.

426   28.   C. F. Lee, C. Y. Liu, R. H. Hsieh and Y. H. Wei, *Annals of the New York*

427   *Academy of Sciences*, 2005, 1042, 246-254.

428   29.   K. Buyukhatipoglu and A. M. Clyne, *Journal of biomedical materials*

429   *research. Part A*, 2011, 96, 186-195.

430   30.   P. L. Apopa, Y. Qian, R. Shao, N. L. Guo, D. Schwegler-Berry, M. Pacurari,

431   D. Porter, X. Shi, V. Vallyathan, V. Castranova and D. C. Flynn, *Particle and*

432   *fibre toxicology*, 2009, 6, 1.

433   31.   M. Lopez-Fanarraga, J. Avila, A. Guasch, M. Coll and J. C. Zabala, *Journal of*

434   *structural biology*, 2001, 135, 219-229.

435   32.   S. Wang, J. Kurepa and J. A. Smalle, *Plant, cell & environment*, 2011, 34,

436   811-820.

437   33.   K. Li, X. Zhao, K. H. B, S. Du and Y. Chen, *ACS nano*, 2013, 7, 9664-9674.

438   34.   A. Dadras, G. H. Riazi, A. Afrasiabi, A. Naghshineh, B. Ghalandari and F.

439   Mokhtari, *Journal of biological inorganic chemistry : JBIC : a publication of*

440   *the Society of Biological Inorganic Chemistry*, 2013, 18, 357-369.

441   35.   M. P. Calatayud, B. Sanz, V. Raffa, C. Riggio, M. R. Ibarra and G. F. Goya,

442   *Biomaterials*, 2014, 35, 6389-6399.

443   36.   M. A. Ojeda-Lopez, D. J. Needleman, C. Song, A. Ginsburg, P. A. Kohl, Y. Li,

444   H. P. Miller, L. Wilson, U. Raviv, M. C. Choi and C. R. Safinya, *Nature*

445   *materials*, 2014, 13, 195-203.

446   37.   M. J. Stevens, *Science*, 2014, 343, 981-982.

447   38.   L. Gonzalez, M. De Santis Puzzonia, R. Ricci, F. Aureli, G. Guarguaglini, F.

448   Cubadda, L. Leyns, E. Cundari and M. Kirsch-Volders, *Nanotoxicology*, 2014,

449   1-8.

450   39.   C. Y. Tay and D. T. Leong, *Nanomedicine (Lond)*, 2014, 9, 2075-2077.

451   40.   D. N. Drechsel, A. A. Hyman, M. H. Cobb and M. W. Kirschner, *Molecular*

452   *biology of the cell*, 1992, 3, 1141-1154.

453   41.   G. T. Bramblett, M. Goedert, R. Jakes, S. E. Merrick, J. Q. Trojanowski and V.

454   M. Lee, *Neuron*, 1993, 10, 1089-1099.

455   42.   U. Wagner, M. Utton, J. M. Gallo and C. C. Miller, *Journal of cell science*,

456   1996, 109 (Pt 6), 1537-1543.

457   43.   M. Horie, K. Nishio, K. Fujita, S. Endoh, A. Miyauchi, Y. Saito, H. Iwahashi,

458   K. Yamamoto, H. Murayama, H. Nakano, N. Nanashima, E. Niki and Y.

459   Yoshida, *Chem Res Toxicol*, 2009, 22, 543-553.

460   44.   H. Suzuki, T. Toyooka and Y. Ibuki, *Environ Sci Technol*, 2007, 41,

461   3018-3024.

462 45. L. L. Shen, W. X. Xu, A. P. Li, J. Ye and J. W. Zhou, *Apoptosis*, 2011, 16,

463   1177-1193.

464 46. Y. Mimori-Kiyosue, N. Shiina and S. Tsukita, *Current biology : CB*, 2000, 10,

465   865-868.

466 47. A. Akhmanova, C. C. Hoogenraad, K. Drabek, T. Stepanova, B. Dortland, T.

467   Verkerk, W. Vermeulen, B. M. Burgering, C. I. De Zeeuw, F. Grosveld and N.

468   Galjart, *Cell*, 2001, 104, 923-935.

469 48. T. Stepanova, J. Slemmer, C. C. Hoogenraad, G. Lansbergen, B. Dortland, C. I.

470   De Zeeuw, F. Grosveld, G. van Cappellen, A. Akhmanova and N. Galjart, *The*

471   *Journal of neuroscience : the official journal of the Society for Neuroscience*,

472   2003, 23, 2655-2664.

473 49. L. Rodriguez-Fernandez, R. Valiente, J. Gonzalez, J. C. Villegas and M. L.

474   Fanarraga, *Acs Nano*, 2012, 6, 6614-6625.

475 50. Y. A. Komarova, I. A. Vorobjev and G. G. Borisy, *J Cell Sci*, 2002, 115,

476   3527-3539.

477 51. H. Y. Du, B. Xu, C. X. Wu, M. Li, F. X. Ran, S. Q. Cai and J. R. Cui, *Acta*

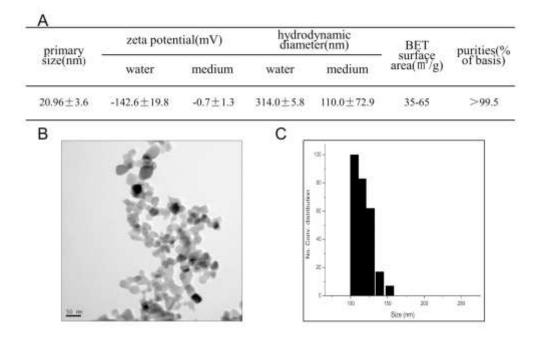478   *Bioch Bioph Sin*, 2012, 44, 136-146.

479

480

481

Figure 1. (A) Characteristic of TiO2 NPs in water and in medium. (B) TEM image of TiO2 NPs, bar=50 nm.
(C) Particle-size distribution of TiO2 NPs prepared in cell culture medium.
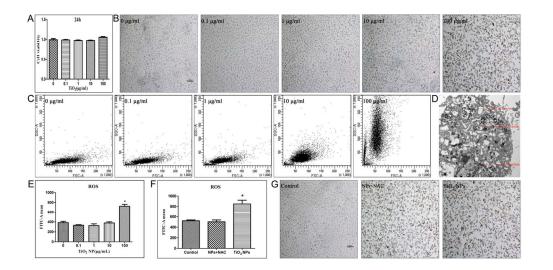121x79mm (300 x 300 DPI)

Figure 2. (A) Cell viability after treated with different concentrations of TiO2 NPs for 24 h. Values were expressed as means ± SE from three separate experiments. (B) SH-SY5Y cells treated with range concentrations of TiO2 NPs. Images were collected in ×100 magnification with light microscope. bar=10 μm. (C) The uptake of TiO2 NPs analyzed by Flow cytometry (FCM). Forward-scatter(ed) (FS) light and side scatter(ed) (SS) light were analyzed of each group treated with NPs. (D) TEM image showed a section of a SY5Y cell treated with NPs. TiO2 NPs were accumulated in lysosomes and cytoplasm as indicated. (E) Cells reactive oxygen species (ROS) formation measured by FCM after TiO2 NPs treatment. Each FITC-mean was compared with control group (P<0.05). Values were expressed as means ± SE from at least three separate experiments. (F) ROS formation measured by FCM after ROS blocking. Control: untreated cells; TiO2 NPs: cells treated with 100 μg/ml TiO2 NPs for 24 h; NPs+NAC: cells treated with TiO2 NPs and incubated with ROS scavenger-NAC. Values were collected and presented as above. (G) Morphology changes after NPs treatment and NAC rescue, bar=10 μm.
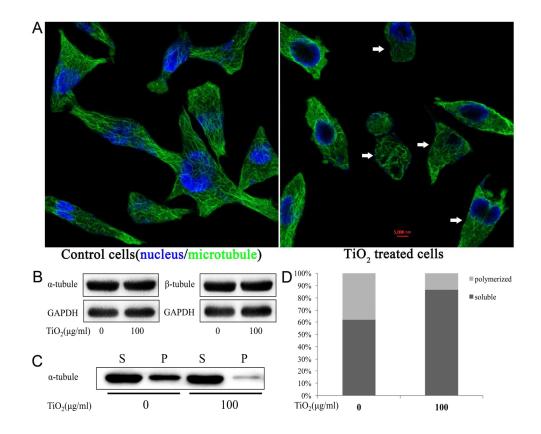
131x67mm (300 x 300 DPI)

Figure 3. (A) Cytoskeleton of SY5Y cells revealed by immunofluorescence and confocal microscope examination. Nucleus was stained blue with DAPI and microtubule was stained green. Control cells showed well organized and extended microtubules, while decreased microtubule density, disorganization, and disruption of microtubules can be observed (white arrow) in TiO2 NPs treated cells. (B) Western blot analysis of the expression of two main microtubule proteins (α-tubule and β-tubule) between control group and NPs treated group. GAPDH was invited as loading control. (C) Western blot analysis of soluble and polymerized tubules in control and treated cells separately, S: soluble, P: polymerized. (D) Quantitative analysis of soluble and polymerized tubules by densitometry with image-J software. Total tubule of each group was considered as 100%.
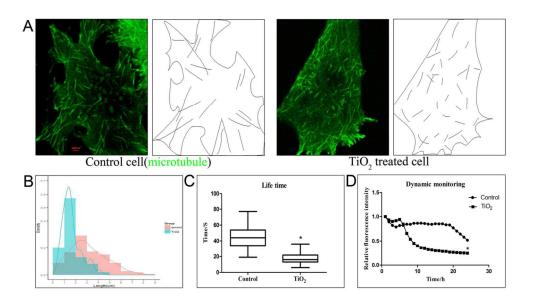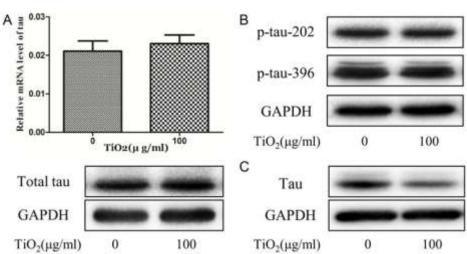192x156mm (300 x 300 DPI)

Figure 4. (A) Trajectory of EB3-GFP labeled de novo microtubules in living cells during about 2 min time lapse. Nascent microtubules were marked with black lines and cellular contours were outlined. (B) Histogram of the length distribution of unbroken microtubules in both groups (n=200 in control cells, n=100 in TiO2 NPs treated cells). (C) Time of each microtubule from merging to disappearance during about 2 min time lapse (n=100) was presented in Boxplot (P<0.01). (D) Dynamic monitoring of steady state of microtubules via the changing of average fluorescence intensity during 24 h continuous observation of the monitored cells (P<0.05). The first time-point fluorescence intensity of each group was standardized as"1". 113x64mm (300 x 300 DPI)

Figure 5. (A) Relative expression of total tau proteins in both mRNA and protein levels between two groups, values were expressed as means ± SE. (B) Phosphorylation status of tau proteins at ser202 and ser396. (C) Western blot analysis of tau in the supernatant after high speed of centrifugation in both control cells and NPs treated cells. GAPDH was invited as mRNA and protein loading control.
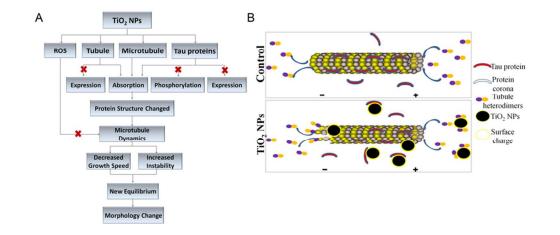68x37mm (300 x 300 DPI)

Figure 6. (A) A simple structure chart to describe our study. Possible passageway are indicated in line with arrow, and excluded passages are marked with fork. (B) Nanoparticles-microtubule-tau interaction model. Microtubule polarity is indicated with the (+) and (-) signs. In normal condition, tubules add to the plus end and depolymerized from minus end at proper speed, Tau proteins bind to the proper site to promote polymerization and stable microtubules. In the presence of TiO2 NPs, tubule heterodimers absorbs to TiO2 NPs, decreases the effective concentration of tubule, TiO2 NPs can also bind to assembled microtubules, affect the electronic environment to sustain microtubule structures. They can absorb tau proteins, which may disturb the normal function of tau and promote the instability of microtubules.
74x33mm (300 x 300 DPI)